全球地震波伝播シミュレーション

課題責任者

坪井誠司　海洋研究開発機構 地球情報基盤センター

著者

坪井誠司*1, Rhett Butler*2

*1 海洋研究開発機構 地球情報基盤センター, *2 University of Hawai‘i

地球内核を通過する地震波の観測波形についてスペクトル要素法を用いた理論地震波形記録を計算し、地球内核表面の構造のモデル化を行った。Butler and Tsuboi (2010)で用いた地震と観測点の組み合わせに加えて震央距離が 179 度より大きい新たな地震と観測点の組み合わせ 39 個に対して地震波形記録を足し合わせる stacking を施した観測波形の再現を試みた。内核表面の低速度構造モデル(Cormier, 2015)に対する理論地震波形記録は観測波形に見られる PKIIKP 波の前駆波を再現しており、内核表面の 3 次元的不均質構造を示唆している。これは地球ダイナモの成因などへも示唆を与えるものである。

キーワード : 数値波形計算、地震波動、地球内核の構造

1. はじめに

地球内核は、地球内部最深部にある固体の領域であり、観測が限られることから、その地震波 S 波速度構造や内格差分回転など現時点でも未解明の事象が多い。特に、内核表面の構造については地球磁場の原因となるダイナモとの関連性からその性質を解明することが重要となる。我々は、これまで Butler and Tsuboi (2010)[1]により地球内核を通過する地震波の観測波形についてモデル化を行ってきた。最近、この観測に新たなデータを加えることが出来たので、平成 30 年度に改めてモデル化を行ったところ、内核表面の地震波低速度不均質構造を加えることで観測波形を良く説明出来ることが分かった。

2. 理論地震波形記録

図 1 は Butler and Tsuboi (2010)[1]で用いた地震震源の対蹠点における地震波 PKIKP と PKIIKP の波線を示したものである。このうち、内核表面で反射する PKIIKP は PKIKP の約 30 秒後に到達する。図 2 には、Butler and Tsuboi (2010)[1]で用いた地震と観測点の組み合わせに対して、PKIIKP が内核表面を通過する領域を図示している。今回、震央距離が 179 度より大きい新たな地震と観測点の組み合わせ 39 個に対して地震波形記録を足し合わせる stacking を施したところ、図 3 に見られる PKIIKP 波の前に到着する波が見られることが分かった。この波を説明するために地球内部地震波速度構造モデルに変更を加え、理論地震波形記録を計算した。理論地震波形記録の計算にはスペクトル要素法のパッケージ specfem を用いた (Komatitsch et al., 2005)[2]。理論地震波形記録計算には ES3 の 7776 コアを用いた。理論地震波形記録の精度は 3.5 秒である。

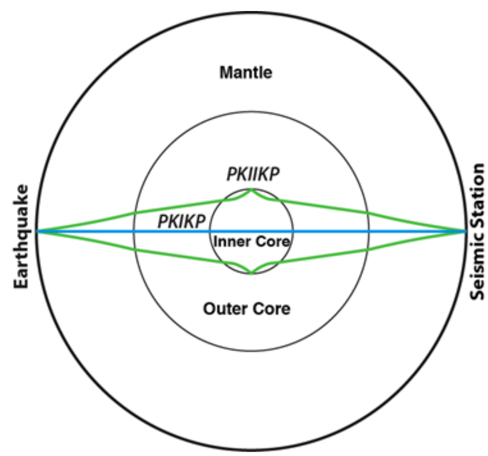

図 1　地震震源の対蹠点における地震波 PKIKP(青)と PKIIKP(緑) の波線。

一次元地球モデルである PREM に対して計算した理論波形記録と図 4 に示した内核表面の低速度構造モデル (Cormier, 2015)[3]に対する理論波形記録を図 3 に比較している。図 3 に示すようにこのモデルによる理論地震波形記録は観測波形に見られる PKIIKP 波の前駆波を再現している。

Butler and Tsuboi (2010)では、別の地震と観測点の組み合わせ(図 2 の赤線で波線を示している）に対し

PKIIKP

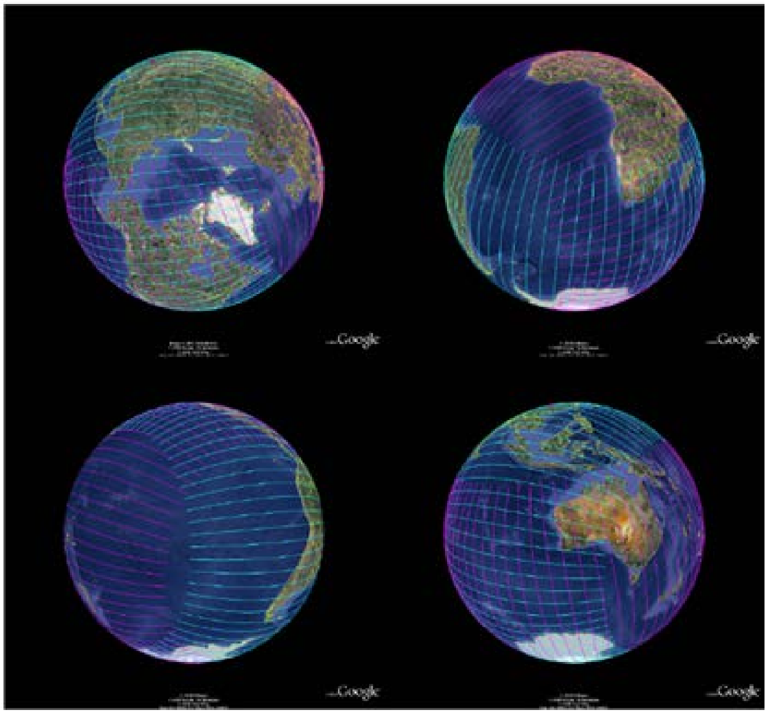

図 2　PKIIKP 波が内核表面を通過する領域(黄色) 赤は別の地震−観測点の組み合わせ。

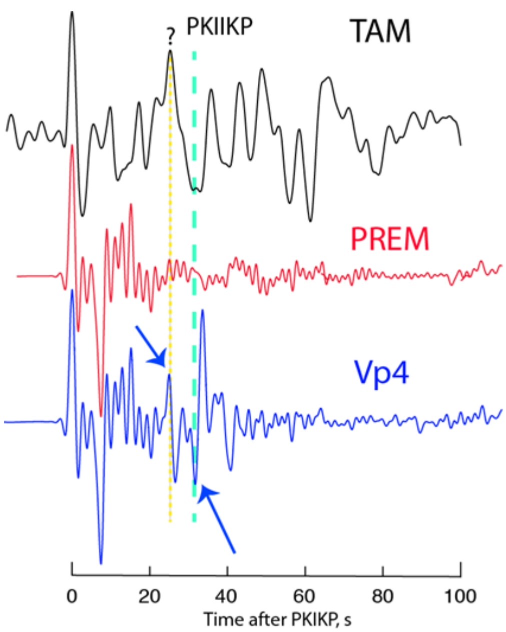

図 3　観測波形の stacking 結果(黒) 、1 次元地球モデルの理論記録(赤)、内核表面の S 波不均質構造を導入した理論記録(青)。

ては PKIIKP 波近辺にはこのような波は見られないことを示しており、図 4 に示した低速度構造は内核表面に局在していることが推察される。

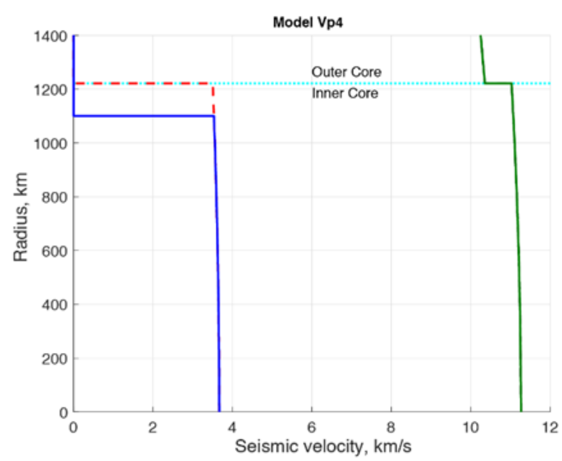

図 4　図 3 で示した理論記録に用いた内核構造モデル。

謝辞

観測波形記録は GEOSCOPE 及び IRIS GSN により得られたものを用いた。理論波形記録の計算には海洋研究開発機構の地球シミュレータを用いた。

文献

[1] Butler, R., and S. Tsuboi (2010), Antipodal seismic observations of temporal and global variation at Earth’s inner-outer core boundary, Geophys. Res. Lett., 37, L11301, doi:10.1029/2010GL042908.

[2] Komatitsch D, Tsuboi S, and Tromp J. (2005) The spectral-element in seismology, in Seismic Earth: Array analysis of broadband seismograms, Geophys. Monograph 157, AGU, pp. 205- 227.

[3] Cormier, V. F. (2015), Detection of inner core solidification from observations of antipodal PKIIKP, Geophys. Res. Lett., 42, doi:10.1002/2015GL065367.

Antipodal Constraints on Earth's Inner-Outer Core Boundary Region

Project Representative
Seiji Tsuboi   Center for Earth Information Science and Technology, Japan Agency for Marine-Earth Science and Technology

Authors
Seiji Tsuboi[*1] Rhett Butler[*2]
[*1]Center for Earth Information Science and Technology, Japan Agency for Marine-Earth Science and Technology, [*2]University of Hawai'i

We model the antipodal arrivals of PKIIKP data by using the spectral element method (SEM) - taking into account 3D variations inside Earth, such as P-wave velocity, S-wave velocity and density, attenuation, anisotropy, ellipticity, topography and bathymetry, and crustal thickness - to compute synthetic seismograms. The initial model used incorporates a simple PREM model for the Core, a 3D tomographic P-wave model for the Earth's Mantle, crustal model CRUST2.0, and topography and bathymetry model ETOPO5 (NOAA). In modeling the antipodal earthquakes, we use a mesh with a total of 13.5 billion global integration grid points, which corresponds to an approximate grid spacing of 2.0 km along the Earth's surface and provides for synthetics seismograms accurate up to 3.5 seconds. The observed unknown seismic phase arrival bounded between PKIKP and PKIIKP indicates structure within the Inner Core. Our working model suggests a liquid-liquid Inner-Outer Core Boundary, and a liquid-solid discontinuity at a radius of 1100 km, or ~120 km below the IOCB.

Keywords: Numerical modelling, Wave propagation, Inner Core structure and heterogeneity

1. Introduction

The Inner and Outer Core regions of Earth have been shown to exhibit many features which relate to the dynamics and evolution of Earth, including anisotropy in the Inner Core [1-14], Inner Core rotation with respect to the Mantle [15-20], degree one variation [21-24],structure within the Inner Core [25-56] and velocity gradients at the base of the Outer Core [57,58]. At the antipode of an earthquake, Earth acts like a nearly spherical lens focusing seismic energy through an axis-symmetric region about the diameter between the earthquake and its antipode (Figure 1). Antipodal observations have the potential to illuminate global Earth structure [59-61; 20, 51] and complement traditional body-wave and free-oscillation seismic methods.

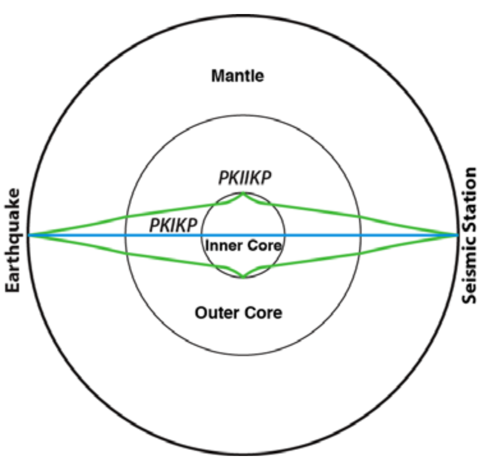

Figure 1. PKIKP and PKIIKP seismic waves both traverse the Inner Core, shown in cross-section. However, the antipodal paths for PKIIKP encompasses all azimuths between the earthquake and its antipode.

2. Data

We have substantially augmented the antipodal data set introduced by Butler and Tsuboi [20], comprising diametral axes between earthquake and antipodal receiving station (*i.e.*, Tonga–Algeria & Chile–China) from 8 earthquakes to 39 in the distance range $\Delta > 179°$. This has enabled data stacking to improve SNR of the Inner Core arrivals. Stacked antipodal data for the Tonga–Algeria diametral axis are shown in Figure 2.

3. Spectral-element Method and Seismic Modeling

We model the data in Figure 2 by using the spectral-element method (SEM) [62,63]—taking into account 3D variations inside Earth, such as P-wave velocity, S-wave velocity and density, attenuation, anisotropy, ellipticity, topography and bathymetry, and crustal thickness—to compute synthetic seismograms. The initial model used incorporates a simple PREM model [64] for the Core, a 3D tomographic P-wave model for the Earth's Mantle, GAP-P1 [65], crustal model CRUST2.0 [66], and topography and bathymetry model ETOPO5 (NOAA). In modeling the antipodal earthquakes, we use a mesh with a total of 13.5 billion global integration grid points, which corresponds to an approximate grid spacing of 2.0 km along the Earth's surface and provides for synthetics seismograms accurate up to 3.5 seconds.

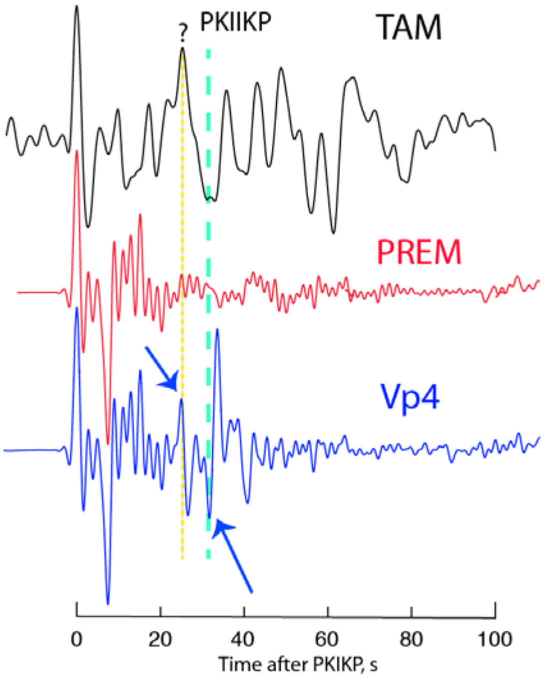

Figure 2. TAM data are compared with PREM and Inner Core model Vp4. The PKIIKP arrival time in aqua, preceded by an unknown Inner Core arrival (**?**) in yellow, are featured in Vp4 (blue arrows) but not PREM. Unlike TAM, data for Chile—China diametral axes are better matched by PREM, indicating substantial lateral heterogeneity in Earth's Inner Core.

4. Inner Core Structure

The TAM unknown seismic phase (**?**) arrival bounded between PKIKP and PKIIKP indicates structure within the Inner Core. The working model Vp4 incorporates a liquid-liquid Inner-Outer Core Boundary [51], and a liquid-solid discontinuity at a radius of 1100 km, or ~120 km below the IOCB (Figure 3).

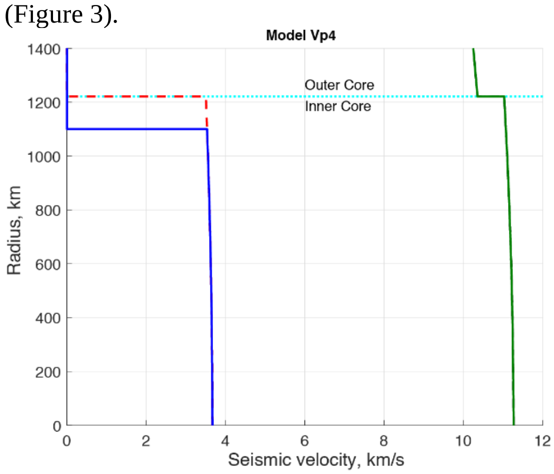

Figure 3. Inner Core velocity profiles for P-waves (green) and S-waves (blue). Dotted red indicates modification from PREM model.

5. Inner Core Sampled

At the antipode the seismic energy converges from all azimuths, and the ray paths join to form a ray-sheet. For PKIIKP each ray-sheet encompasses nearly 60% of the ICB, By incorporating other diametral axes, nearly 99% of the uppermost Inner Core is sampled by the antipodal propagation surfaces. This is illustrated in Figure 4 where Tonga–Algeria paths (TAM) are projected to the Earth's surface along with Chile–China paths (which are reasonably fit by PREM).

PKIIKP

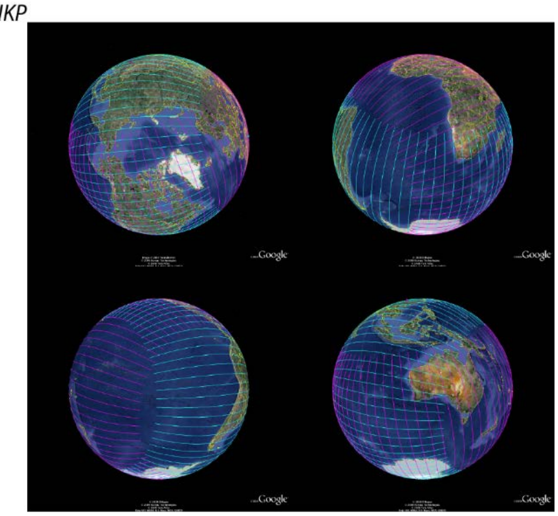

Figure 4. Antipodal coverage of the top of the Inner Core. The antipodal propagation ray-surface Fresnel zone for PKIIKP at the top of Inner Core is projected to the Earth's surface for the TAM (in cyan) and Chile-China (in magenta) diametral axes. Each annulus surface is illustrated by individual ray- paths from source to receiver, shown at 5° increments. The upper left orthographic projections is centered on the quasi-Eastern hemisphere (0°, 110°E) noted in Inner Core studies [Tanaka and Hamaguchi, 1997[21]; Niu and Wen, 2001[22]]; other projections are perspectives corresponding to 120° rotations for a circumscribed tetrahedron. The two ray surfaces for PKIIKP for these events encompass most of the Inner Core. The TAM ray-surface also corresponds to the region wherein a (rotational ?) time shift in PKIIKP is manifested. Map adapted from GoogleEarth© with permission.

6. Conclusion

Progress is being made in documenting and explaining non-radial structure within the Inner Core by using a unique antipodal data set. The next phase of analysis will incorporate 3D structure within the Inner Core to simultaneously model the Tonga–Algeria path with Chile–China paths.

Acknowledgement

We used seismic data provided by Geoscope and the Global Seismographic Network. Computations were conducted on the Earth Simulator at the Japan Agency for Marine-Earth Science and Technology.

References

[1] Poupinet, G., R. Pillet, and A. Souriau (1983), Possible heterogeneity of the Earth's core deduced from PKIKP travel times, *Nature, 305*, 204–206.

[2] Woodhouse, J. H., D. Giardini, and X.-D. Li (1986), Evidence for inner core anisotropy from splitting in free oscillation data, *Geophys. Res. Lett., 13*, 1549–1552.

[3] Morelli, A., A. M. Dziewonski , and J. H. Woodhouse (1986), Anisotropy of the core inferred from PKIKP travel times, *Geophys. Res. Lett., 13*, 1545–1548.

[4] Creager, K.C. (1992), Anisotropy of the inner core from differential travel times of the phases PKP and PKIKP, *Nature*, *356*, 309–314.

[5] Tromp, J. (1993), Support for anisotropy of the Earth's inner core from free oscillations, *Nature*, *366*, 678–681.

[6] Song, X., and D. V. Helmberger (1993), Anisotropy of Earth's inner core, *Geophys. Res. Lett., 20*, 2591–2594.

[7] Shearer, P. M. (1994), Constraints on inner core anisotropy from ISC PKP(DF) travel times, *J. Geophys. Res., 99*, 19647–19659.

[8] Souriau, A., and Romanowicz, B., 1996. Anisotropy in inner core attenuation: a new type of data to constrain the nature of the solid core, Geophys. Res. Lett., 23(1), 1-4.

[9] Ishii, M., and A. M. Dziewonski (2002), The innermost inner core of the Earth: evidence for a change in anisotropic behavior at the radius of about 300 km, *Proc. Natl. Acad. Sci. U.S.A., 22*, 14026–14030.

[10] Niu, F., and Qi-Fu Chen (2008), Seismic evidence for distinct anisotropy in the innermost inner core, *Nature Geoscience, 1*, 692–696.

[11] Niu, F., and Q.-F. Chen (2010), Seismic evidence for distinct anisotropy in the innermost inner core, Nat. Geosci., 314, 692–696, doi:10.1038/ngeo314.

[12] Irving, J.C.E., and Deuss, A., 2011. Stratified anisotropic structure at the top of Earth's inner core: A normal mode study, Phys. Earth Planet. Inter., 186, 59-69, doi:10.1016/j.pepi.2011.03.003

[13] Wang, T., Song, X., and Xia, H. H., 2015. Equatorial anisotropy in the inner part of the Earth's inner core from autocorrelation of earthquake coda, Nat. Geosci., 8, 224–227, doi:10.1038/NGEO2354.

[14] Frost, D. and Romanowicz, B., 2017. Constraints on inner core anisotropy using array observations of P'P', Geophys. Res. Lett., 44, https://doi.org/10.1002/2017GL075049

[15] Song, X., and P. G. Richards (1996), Seismological evidence for differential rotation of the Earth's inner-core, *Nature*, *382*, 221–224.

[16] Creager, K. C. (1997), Inner core rotation rate from small-scale heterogeneity and time-varying travel times, *Science*, *278*, 1284–1288.

[17] Song, X. (1997), Anisotropy of Earth's inner core, Rev. Geophys., 35(3), 297–313.

[18] Laske, G., and G. Masters (1999), Limits on differential rotation of the inner core from an analysis of the Earth's free oscillations, *Nature*, *402*, 66–68.

[19] Zhang, J., X. Song, Y. Li, P. G. Richards, X. Sun, and F. Waldhauser (2005), Inner core differential motion confirmed by earthquake waveform doublets, Science 309, 1357–1360.

[20] Butler, R., and S. Tsuboi (2010), Antipodal seismic observations of temporal and global variation at Earth's inner-outer core boundary, Geophys. Res. Lett., 37, L11301, doi:10.1029/2010GL042908.

[21] Tanaka, S., and H. Hamaguchi (1997), Degree one heterogeneity and hemispherical variation of anisotropy in the inner core from PKP(BC) and PKP(DF) times, *J. Geophys. Res.*, *102*, 2925–2938.

[22] Niu, F., and L. Wen (2001), Hemispherical variations in seismic velocity at the top of the Earth's inner-core, *Nature, 410*, 1081–1084.

[23] Waszek, L., and A. Deuss (2011), Distinct layering in the hemispherical seismic velocity structure of Earth's upper inner core, J. Geophys. Res., 116, B12313, doi:10.1029/2011JB008650.

[24] Miller, M.S., Niu, F., Vanacore, E.A., 2013. Aspherical structural heterogeneity within the uppermost inner core: insights into the hemispherical boundaries and core formation. Phys. Earth Planet. Inter. 223, 8–20. http://dx.doi.org/10.1016/j. pepi.2013.02.001

[25] Lehmann, Inge (1936). P'. Publications du Bureau Central Séismologique International. A14 (3): 87–115.

[26] Dziewonski, A. M., and F. Gilbert (1971), Solidity of the inner core of the Earth inferred from normal mode observations, Nature, 234, 465 – 466.

[27] Cummins, P. and Johnson, L.R., 1988a. Short-period body wave constraints of properties of the Earth's inner core boundary, J. Geophys. Res., 93, 9058–9074.

[28] Cummins, P. and Johnson, L.R., 1988b. Synthetic seismograms for an inner core transition of finite thickness, Geophys. J., 94, 21-34.

[29] Song, X., and D. V. Helmberger (1998), Seismic evidence for an inner core transition zone, *Science*, *282*, 924–927.

[30] Vidale, J. E. and Earle, P.S., 2000. Fine-scale heterogeneity in the Earth’s inner core, Nature, 404, 273-275.

[31] Deuss, A., J. H. Woodhouse, H. Paulssen, and J. Trampert (2000), The observation of inner core shear waves, Geophys. J. Int., 142(1), 67–73, doi:10.1046/j.1365-246x.2000.0147x.

[32] Wen, L., and F. Niu (2002), Seismic velocity and attenuation structures in the top of the Earth’s inner core, *J. Geophys. Res.*, *107*, 2273, doi:10.1029/2001JB000170.

[33] Cormier, V. F., and X. Li (2002), Frequency dependent attenuation in the inner core: Part II. A scattering and fabric interpretation, J. Geophys. Res., 107(B12), 2362, doi:10.1029/2002JB001796.

[34] Stroujkova, A., and V. F. Cormier (2004), Regional variations in the uppermost 100 km of the Earth’s inner core, *J. Geophys. Res.*, *109*, B10307, doi:10.1029/2004JB002976.

[35] Koper, K. D., Franks, J.M., and Dombrovskaya, M., 2004. Evidence for small-scale heterogeneity in Earth’s inner core from a global study of PKiKP coda waves, Earth Planet. Sci. Lett., 228, 227-241.

[36] Cao, A., and B. Romanowicz (2004), Constraints on the density and shear velocity contrasts at the inner core boundary, Geophys. J. Int., 157, 1–6.

[37] Koper, K. D. and Dombrovskaya, M., 2005. Seismic properties of the inner core boundary from PKiKP/P amplitude ratios, Earth Planet Sci. Lett., 237, 680-694.

[38] Leyton, F., K. D. Koper, L. Zhu, and M. Dombrovskaya, 2005. On the lack ofseismic discontinuities within the inner core, Geophy. J. Inter., 162, 779–786,.

[39] Kawakatsu, H., 2006. Sharp and seismically transparent inner core boundary region revealed by an entire network observation of near vertical PKiKP, Earth Planets Space, 58, 855-863

[40] Leyton, F., and K. D. Koper (2007), Using PKIKP coda to determine inner core structure: 2. Determination of QC , J. Geophys. Res., 112, B05317, doi:10.1029/2006JB004370.

[41] Deguen, R., Alboussière, T. and Brito, D., 2007. On the existence and structure of a mush at the inner core boundary of the Earth. Physics of the Earth and Planetary Interiors, 164(1-2), pp.36-49.

[42] Zou, Z., K. D. Koper, and V. F. Cormier (2008), The structure of the base of the outer core inferred from seismic waves diffracted around the inner core, *J. Geophys. Res.*, *113*, B05314,

[43] Cao, A., and Romanowicz, B., 2009. Constraints on shear wave attenuation in the Earth’s inner core from an observation of PKJKP, Geophys. Res. Lett., 36, L09301, doi:10.1029/2009GL038342.

[44] Tkalcic, H., B. L. N. Kennett, and V. F. Cormier (2009), On the inner-outer core density constrast from PKIKP/PcP amplitude ratios and uncertainties caused by seismic noise, Geophys. J. Int., 179(1), 425–443, doi:10.1111/j.1365-246s.2009.04294x.

[45] Monnereau, M., M. Calvet, L. Margerin, and A. Souriau (2010), Lopsided growth of Earth’s inner core, Science, 382, 1015–1017, doi:10.1126/science.1186212.

[46] Cormier, V.F., Attanayake, J., and He, K., 2011. Inner core freezing and melting: Constraints from seismic body waves, Phys. Earth. Planet. Inter., 188(3-4), 163-172, doi: 10.1016/j.pepi.2011.07.007.

[47] Ohtaki, T., Kaneshima, S., and Kanjo, K., 2012. Seismic structure near the inner core boundary in the south polar region, J. Geophys. Res., 117, B03312, doi:10.1029/2011JB008717.

[48] Cormier, V.F. and Attanayake, J., 2013. Earth’s solid inner core: Seismic implications of freezing

and melting. Journal of Earth Science, 24(5), pp.683-698.

[49] Attanayake, J., V. F. Cormier, and S. deSilva (2013), Uppermost inner core seismic structure—new insights from body waveform inversion, Earth Planet. Sci. Lett., 385, 49–58.

[50] Attanayake, J., Cormier, V.F., and deSilva, S.M., 2014. Uppermost inner core seismic structure – new insights from body waveform inversion, Earth. planet. Sci. Lett., 385, 49–58.

[51] Cormier, V. F. (2015), Detection of inner core solidification from observations of antipodal PKIIKP, Geophys. Res. Lett., 42, doi:10.1002/2015GL065367.

[52] de Silva, S., Cormier, V.F., Zheng, Y., 2017. Inner Core Boundary Topography Explored with Reflected and Diffracted P waves, Phys. Earth planet. Inter., doi: http://dx.doi.org/10.1016/j.pepi.2017.04.008

[53] Tian, D., and Wen, L., 2017. Seismological evidence for a localized mushy zone at the Earth's inner core boundary, Nat. Comm., 8:165, doi:10.1038/s41467-017-00229-9

[54] Pejić, T., Tkalčić, H., Sambridge, M., Cormier, V. F., and Benavente, R.,2017. Attenuation tomography of the upper inner core, J. Geophys. Res. Solid Earth, 122, 3008–3032, doi:10.1002/2016JB013692.

[55] Attanayake, J., Thomas, C., Cormier, V.F., Miller, M.S. and Koper, K.D., 2018. Irregular Transition Layer Beneath the Earth's Inner Core Boundary From Observations of Antipodal PKIKP and PKIIKP Waves. *Geochemistry, Geophysics, Geosystems*, *19*(10), pp.3607-3622.

[56] Adam, J.M.-C., Ibourichène, A., Romanowicz, B., 2018. Observation of core sensitive phases: Constraints on the velocity and attenuation profile in the vicinity of the inner-core boundary, Phys. Earth Planet. Inter., 275, 19-31, https://doi.org/10.1016/j.pepi.2017.12.008.

[57] Song, X. and D. V. Helmberger (1995), A P wave velocity model of Earth's core, *J. Geophys. Res., 100*, 9817–9830.

[58] Yu, W., L. Wen, and F. Niu (2005), Seismic velocity structure in the Earth's outer core, *J. Geophys. Res., 110*, B02302, doi:10.1029/2003JB002928.

[59] Rial, J. A. (1979), Seismic waves at the epicenter's antipode, Doctoral Dissertation Caltech, Pasadena.

[60] Rial, J. A., and V. F. Cormier (1980), Seismic waves at the epicenter's antipode, *J. Geophys. Res., 85*, 2661–2668.

[61] Butler, R. (1986), Amplitudes at the antipode, *Bull. Seismo. Soc. Am., 76***,** 1355–1365.

[62] Komatitsch, D., and J. P. Vilotte (1998), The spectral-element method: an efficient tool to simulate the seismic response of 2D and 3D geological structures, *Bull. Seismol. Soc. Am., 88*, 368–392.

[63] Komatitsch, D., J. Ritsema, and J. Tromp (2002), The spectral-element method, Beowulf computing, and global seismology, *Science, 298*, 1737–1742.

[64] Dziewonski, A. M., and D. L. Anderson (1981), Preliminary reference Earth model, *Phys. Earth Planet. Inter., 25*, 297–356.

[65] Obayashi, M., H. Sugioka, J. Yoshimitsu, and Y. Fukao (2006), High tem- perature anomalies oceanward of subducting slabs at the 410-km discon- tinuity, *Earth Planet. Sci. Lett.*, 243, 149–158, doi:10.1016/j.epsl.2005. 12.032.

[66] Bassin, C., G. Laske, and G. Masters (2000), The current limits of resolution for surface wave tomography in North America, Eos Trans. AGU, 81, F897.